The fibre pull-out energy of misaligned short fibre composites

SHAO-YUN FU, BERND LAUKE
Institute for Polymer Research Dresden e.V., Hohe Strasse 6, 01069 Dresden, Germany

A theoretical study on the fibre pull-out energy has been carried out for short fibre-reinforced composites. Two probability density functions were introduced for modelling the fibre-length distribution and the fibre-orientation distribution. By taking into account the effect of snubbing friction between fibres and matrix at the fibre exit point during fibre pull-out, and that of the fracture stress of fibres obliquely crossing the fracture plane (i.e. the inclined strength of fibres), the fibre pull-out energy of composites has been derived as a function of fibre-length distribution and fibre-orientation distribution, as well as interfacial properties. The previously existing fibre pull-out energy theories can be deduced from the present model. The effects of fibre-length distribution, fibre-orientation distribution, interfacial properties, snubbing-friction coefficient and parameter A for determining the inclined strength of fibres on the fibre pull-out energy, have been studied in detail. The present study provides the necessary information as to which fibre-length distribution, fibre-orientation distribution and interfacial property are required to achieve a desired fibre pull-out energy and hence a desired composite toughness. High-strength fibres, a large fibre-volume fraction and a large fibre diameter for a comparatively large mean fibre length, are shown to be favourable for achieving a high fibre pull-out energy.

1. Introduction

Short fibre-reinforced composites have many applications as engineering materials. Fracture resistance is one important property of engineering materials, and a measure of fracture resistance is given by the specific work of fracture, or the fracture toughness. Kim and Mai [1] have recently given a comprehensive review of the fracture toughness of fibre composites. It has been indicated that the fracture toughness of composites depends not only on the properties of constituents but also significantly on the bonding efficiency across the interface. For short fibre composites, the failure mechanisms can be concluded from the literature [1–8] and are listed as follows: (1) fibre–matrix interfacial debonding, (2) post-debonding friction, (3) matrix plastic deformation, (4) fibre plastic deformation, (5) fibre fracture, (6) matrix fracture, (7) fibre pull-out. However, it is not necessary for all these failure mechanisms to operate simultaneously for a given fibre–matrix system, and in some composites, one of these toughness contributions may dominate the total fracture toughness of short fibre composites. For brittle fibre–brittle matrix systems, the toughness contribution of fibre pull-out is the principal term [7]. For brittle fibre–ductile matrix systems, the matrix deformation is constrained due to the presence of fibres, especially when the content of fibres in the composites is high [9], the brittle fracture of ductile matrices was observed in the injection-moulded short glass fibre-reinforced thermoplastics [10], hence the toughness contribution of the matrix is seriously limited. On the other hand, for injection-moulded glass fibre-reinforced thermoplastics, the most important energy-absorbing mechanism related to short fibres is that of fibre pull-out [9]; for injection-moulded long glass fibre-reinforced polyamide 6, fibre pull-out has been indicated to be the major energy-absorbing mechanism in the composite [11]. So the fibre pull-out is one important energy-absorbing mechanism for brittle discontinuous fibre–ductile matrix composites. For a ductile fibre–brittle matrix system, e.g. nickel and steel fibre-reinforced cements, fibre pull-out has also been indicated to be the dominant failure mechanism [12]. From this short review, it becomes clear that the fibre pull-out mechanism is the important one for the short fibre-reinforced composites mentioned above. Moreover, it was pointed out that the main source of fracture toughness of most high-performance composites is fibre pull-out energy [1]. However, Lauke *et al.* [2] considered the fracture process of comparatively ductile thermoplastics composites with aligned glass fibres of subcritical transfer length. Under static loading conditions, intensive plastic flow occurs locally in the matrix and the contribution of matrix to the work of fracture in this case is predominant; a similar phenomenon was observed by Gupta *et al.* [8] for short glass fibre-reinforced polypropylene with most fibres of subcritical length. Consequently, the following question has to be answered: what factors influence the fibre pull-out energy and under what circumstances will the fibre pull-out energy be high enough for a given fibre–matrix system, and hence the fracture toughness of composites, to be improved considerably through enhancing the fibre pull-out energy by controlling the factors? To find the answer, a proper fibre pull-out energy theory is required.

For unidirectional short fibre composites, all the fibres are pulled out when the fibre length, L, is less than the critical transfer length, L_c

$$L_c = \sigma_{fu} d_f/(2\tau_i) \quad (1)$$

where σ_{fu} is the tensile strength of fibres which align in the loading direction, τ_i the interfacial shear stress, d_f the fibre diameter.

Assuming the fibre pull-out length, L_{po}, varies between 0 and $L/2$ with a mean value of $L/4$, the fibre pull-out energy, w_{po} (normalized by the fracture plane), is given by [1, 13, 14]

$$w_{po} = \frac{V_f \tau_f L^2}{6d_f} \qquad \text{for } L < L_c \quad (2)$$

where τ_f is the interfacial frictional shear stress and it is assumed to be a constant; V_f is the fibre volume fraction, w_{po} is the maximum when $L = L_c$, i.e.

$$w_{po} = \frac{V_f \tau_f L_c^2}{6d_f} \qquad \text{for } L = L_c \quad (3)$$

If the fibres are of a length greater than L_c, the fraction of fibres which are pulled out will then be L_c/L (on the basis of normal probability) and L_{po} ranges from 0 to $L_c/2$. Hence w_{po} becomes

$$w_{po} = \frac{V_f \tau_f L_c^2}{6d_f}\left(\frac{L_c}{L}\right) \qquad \text{for } L > L_c \quad (4)$$

When there is a distribution of fibre lengths, the fibre pull-out energy can be expressed as follows [8, 15]

$$w_{po} = \frac{\tau_f}{6d_f}\sum_{L_i \leqslant L_c} V_i L_i^2 + \frac{\tau_f L_c^3}{6d_f}\sum_{L_j > L_c}\frac{V_j}{L_j} \quad (5)$$

The first summation refers to subcritical fibres ($L < L_c$) and the second to supercritical fibres ($L > L_c$). L_i and L_j are the fibre lengths of subcritical and supercritical fibres, respectively; V_i and V_j denote the subfractions of sub- and supercritical fibres, respectively.

For non-undirectional composites with short fibres of a constant length, the fibre pull-out energy was studied by Jain and Wetherhold [6, 7]. The effect of snubbing friction between fibres and matrix at the fibre exit point was taken into account when the fibres obliquely cross the fracture plane. The interfacial friction shear stress is assumed in the following form [6, 16]

$$\tau_f(\delta) = a_0 + a_1\delta + a_2\delta^2 \quad (6)$$

where a_0, a_1 and a_2 are constants, determined empirically; δ is the crack-opening displacement of composites. If the pull-out force in the shorter segment exceeds the minimum force to pull out the longer segment, the longer segment will actually pull out; if longer embedded segments do not pull-out, the following conditions should be satisfied [6, 16]

$$a_1 \leqslant a_0/(L/2) \quad (7)$$

$$a_2 \leqslant a_0/(L/2)^2 \quad (8)$$

The fibre pull-out energy can be expressed as

$$w_{po} = \frac{1}{2}\left(\frac{L}{2}\right)^2 \frac{V_f}{A_f}\pi d_f\left[\frac{1}{3}a_0 + \frac{a_1}{12}\left(\frac{L}{2}\right) + \frac{a_2}{30}\left(\frac{L}{2}\right)^2\right] \times [\exp(\mu\theta)\cos\theta] \qquad \text{for } L \leqslant L_c\exp(-\mu\pi/2) \quad (9a)$$

$$w_{po} = \frac{1}{2}\left(\frac{L}{2}\right)^2 \frac{V_f}{A_f}\pi d_f\left(\left[\frac{1}{3}a_0 + \frac{a_1}{12}\left(\frac{L}{2}\right) + \frac{a_2}{30}\left(\frac{L}{2}\right)^2\right] \times N_1[\exp(\mu\theta)\cos\theta] + \left\{\frac{1}{3}a_0\left(\frac{2L_c}{L}\right)^3 N_2[\exp(-2\mu\theta)\cos\theta] + \frac{a_1}{12}\left(\frac{L}{2}\right)\left(\frac{2L_c}{L}\right)^4 N_2[\exp(-3\mu\theta)\cos\theta] + \frac{a_2}{30}\left(\frac{L}{2}\right)^2\left(\frac{2L_c}{L}\right)^5 N_2[\exp(-4\mu\theta)\cos\theta]\right\}\right) \qquad \text{for } L_c\exp(-\mu\pi/2) < L < L_c \quad (9b)$$

$$w_{po} = \frac{1}{2}\left(\frac{L}{2}\right)^2 \frac{V_f}{A_f}\pi d_f\left\{\frac{1}{3}a_0\left(\frac{2L_c}{L}\right)^3\langle\exp(-2\mu\theta)\cos\theta\rangle + \frac{a_1}{12}\left(\frac{L}{2}\right)\left(\frac{2L_c}{L}\right)^4\langle\exp(-3\mu\theta)\cos\theta\rangle + \frac{a_2}{30}\left(\frac{L}{2}\right)^2\left(\frac{2L_c}{L}\right)^5\langle\exp(-4\mu\theta)\cos\theta\rangle\right\} \qquad \text{for } L \geqslant L_c \quad (9c)$$

where A_f is the cross-sectional area of fibre, μ the snubbing-friction coefficient which is defined by Li *et al.* [17], and θ the angle between fibre axis and the loading direction. Also

$$N_1[\ ] = \int_{\theta=0}^{\ln(2L_c/L)/\mu} [\ ]\sin\theta h(\theta)\,d\theta \quad (10)$$

$$N_2[\ ] = \int_{\ln(2L_c/L)/\mu}^{\pi/2} [\ ]\sin\theta h(\theta)\,d\theta \quad (11)$$

$$\langle\exp(\ )\cos\theta\rangle = \int_{\theta=0}^{\pi/2} (\ )\sin\theta h(\theta)\,d\theta \quad (12)$$

where $h(\theta)$ is a probability per unit area on a hemisphere.

Wetherhold and Jain [6, 7] only considered the fibre-orientation distribution, the fibre-length distribution was not taken into account. However, for the extruded and injection-moulded fibre composites, there is not only a fibre-orientation distribution but also a fibre-length distribution in the final product [18–26]. In addition, for the fibre-orientation distribution, only several special cases (aligned and uniform distribution ones) were discussed [6, 7]; a general formula of fibre-orientation distribution was not given. When a fibre is pulled out at an angle with respect to the loading direction, the fracture stress of fibres is reduced because of the flexural stress resulting from the fibre curvature close to the crack faces [27–30]. The fracture stress of oblique fibres is also called the inclined strength of fibres [29], which has been indicated to be a very important fibre parameter; however, it was neglected by Jain and Wetherhold [6, 7].

In the present study, two probability density functions were introduced for modelling the fibre-length and fibre-orientation distributions. The fibre pull-out energy has been derived as a function of fibre-length and fibre-orientation distributions and the interfacial properties by considering the snubbing-friction effect and the inclined fibre-strength effect. All the factors that influence the fibre pull-out energy have been discussed in detail, so that the necessary information can be provided to achieve a high fibre pull-out energy and hence a high fracture toughness of composites for a given fibre/matrix system.

2. Theory

2.1. Fibre-length distribution

During the extrusion and injection-moulding processes, the shear stresses exerted by the screw or ram will break the fibres and result finally in a fibre-length distribution with an asymmetric character with a tail at the long fibre end [24, 31, 32]. As was done in predicting the tensile strength of injection-moulded short fibre-reinforced polymers [33], the fibre-length distribution can be described with a probability density function. Let us define the fibre length probability density function $f(L)$ so that $f(L)\,\mathrm{d}L$ and $F(L)$ are the probability density that the length of fibre is between L and $L + \mathrm{d}L$ and the probability that the length of a fibre is less than or equal to L, respectively. Then the relation to $f(L)$ and $F(L)$ is

$$F(L) = \int_0^L f(x)\,\mathrm{d}x \tag{13a}$$

and

$$\int_0^\infty f(x)\,\mathrm{d}x = 1 \tag{13b}$$

A two-parameter Weibull distribution function has been proposed for modelling the fibre-length distribution and was verified to be effective in describing the density distribution of short glass fibre-reinforced polypropylene [24]

$$f(L) = (m/n)(L/n)^{m-1}\exp[-(L/n)^m] \qquad \text{for } L > 0 \tag{14}$$

where m and n are shape parameters. Ulrych *et al.* [31] gave another form of Weibull distribution, i.e. the so-called Tung's distribution

$$f(L) = abL^{b-1}\exp(-aL^b) \qquad \text{for } L > 0 \tag{15}$$

where a and b are size and shape parameters, respectively. Inserting $b = m$ and $a = n^{-m}$ into Equation 15, it then becomes the same as Equation 14. Also, Equation 15 has been successfully used for describing the fibre-length distribution in short glass fibre-reinforced polyamide (SFRP) [31]. So, in our study we adopted this probability density function and prefer the form of Equation 15 as the fibre length distribution function of SFRP because it looks simple. Therefore, the cumulative distribution function, $F(L)$, can be given by Equations 13 and 15

$$F(L) = 1 - \exp(-aL^b) \qquad \text{for } L > 0 \tag{16}$$

From Equation 15 we can obtain the mean fibre length (i.e. the number average fibre length)

$$\bar{L} = \int_0^\infty Lf(L)\,\mathrm{d}L = a^{-1/b}\Gamma(1/b + 1) \tag{17}$$

where $\Gamma(x)$ is the gamma function. The most probable length (mode length), L_{mod}, can be obtained by differentiating Equation 15 and letting the resultant equation be equal to zero

$$L_{\mathrm{mod}} = \left(\frac{1}{a} - \frac{1}{ab}\right)^{1/b} \tag{18}$$

2.2. Fibre-orientation distribution

During extrusion compounding and injection-moulding processes, progressive and continuous changes in fibre orientation throughout the moulded components take place. The changes are related in a complex way to the size and concentration of fibres, the flow behaviour of melted polymer matrix, the mould cavity and the processing conditions. An orientation distribution generally requires a three-dimensional description. However, it will be shown that only the orientation angle (θ) between the fibre axis and the fracture plane normal (or loading direction) needs to be considered for evaluating the fibre pull-out energy. A fibre-orientation distribution function, representing the orientation angle, must have the property such that the variation of its shape parameters is able to describe a change from a unidirectional distribution to a random distribution.

Let us define a fibre-orientation density function, $g(\theta)$, such that $g(\theta)\,\mathrm{d}\theta$ is the probability density that the orientation of a fibre is between θ and $\theta + \mathrm{d}\theta$. With this assumption, Xia *et al.* [23] proposed a two-parameter exponential function to describe the fibre-orientation distribution in the injection-moulded specimens. Similar to this definition of Xia *et al.*'s fibre-orientation distribution function, the fibre-orientation distribution function is given as follows

$$g(\theta) = [\sin(\theta)]^{2p-1}[\cos(\theta)]^{2q-1} \Big/ \int_{\theta_{\min}}^{\theta_{\max}} [\sin(\theta)]^{2p-1}[\cos(\theta)]^{2q-1}\,\mathrm{d}\theta \tag{19}$$

where p and q are the shape parameters which can be used to determine the shape of the distribution curve, and $p \geqslant 1/2$ and $q \geqslant 1/2$. Also, $0 \leqslant \theta_{\min} \leqslant \theta \leqslant \theta_{\max} \leqslant \pi/2$. The mean fibre orientation, θ_{mean}, can be derived from Equation 19 as

$$\bar{\theta} = \int_{\theta_{\min}}^{\theta_{\max}} \theta g(\theta)\,\mathrm{d}\theta \tag{20}$$

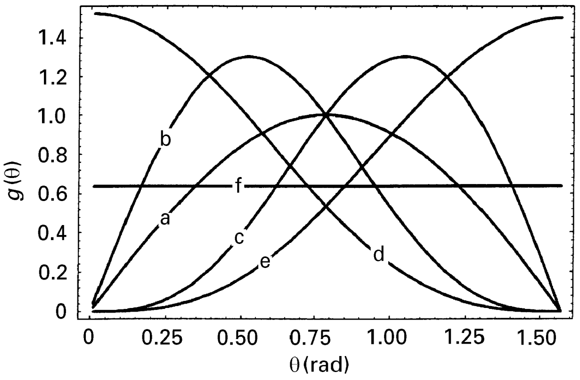

Figure 1 Fibre-orientation distribution curves: (a) $p = q = 1$;. (*b*) $p = 1$, $q = 2$; (c) $p = 2$, $q = 1$; (d) $p = 1/2$, $q = 2$; (e) $p = 2$, $q = 1/2$; (f) $p = q = 1/2$.

Differentiating Equation 19 and letting the resultant equation be zero, we then obtain

$$\theta_{mod} = \arctan\{[(2p-1)/(2q-1)]^{1/2}\} \tag{21}$$

Equation 21 represents the most probable fibre-orientation angle. If $p = q = 1$, $\theta_{mod} = \pi/4$; if $p = 1$ and $q > 1$, then $\theta_{mod} < \pi/4$; if $p > 1$ and $q = 1$, then $\theta_{mod} > \pi/4$; if $p = 1/2$, $\theta_{mod} = 0$; if $q = 1/2$, then $\theta_{mod} = \pi/2$; if $p = q = 1/2$, then there is no θ_{mod} and the fibres distribute randomly; the corresponding fibre orientation distribution curves are shown in Fig. 1. If $p = 1/2$, large q indicates that fibres have a major preferential alignment parallel to the $\theta = 0$ direction; for example, if $q = 100$, the mean fibre-orientation angle is evaluated to be 0.056. If $q = 1/2$, large p indicates that fibres have a major preferential orientation normal to the $\theta = 0$ direction; for example, if $p = 100$, the mean fibre-orientation angle is evaluated to be 1.514. So, all the cases of fibre-orientation distribution are included in Equation 19, thus it is a suitable probability density function for describing the fibre-orientation distribution and will be used in the present study.

The fibre orientation coefficient, f_θ, can be defined as follows [33, 34]

$$f_\theta = 2\int_{\theta_{min}}^{\theta_{max}} g(\theta)\cos^2(\theta)\,d\theta - 1 \tag{22}$$

For $f_\theta = -1$, all fibres lie perpendicular to the fracture-plane normal or loading direction; f_θ = zero corresponds to a random distribution; $f_\theta = 1$ implies all fibres are aligned parallel to the loading direction.

2.3. Pull-out energy for a single misaligned fibre

To evaluate the fibre pull-out energy of short fibre composites, the fibre pull-out load and crack-opening displacement should be predicted. We assume that only the shorter embedded length, l, will pull out, the longer segment length $(L - l)$ will not pull out. The interfacial frictional shear stress, $\tau_f(\delta)$, is assumed to have the same form as Equation 6. If $a_1 = 0$ and $a_2 = 0$, it is a constant interfacial frictional shear stress case. Fig. 2 shows the pull-out of a single fibre with

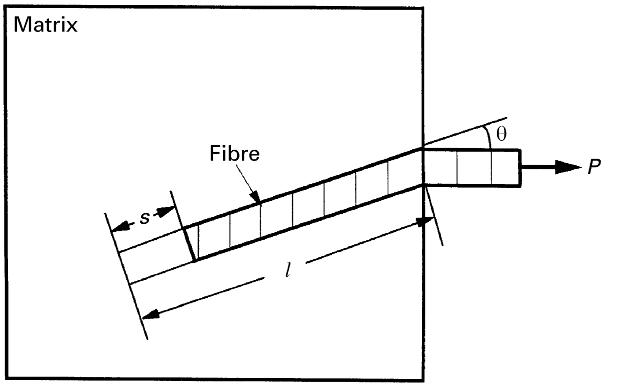

Figure 2 Pull-out of an oblique fibre from a matrix.

shorter embedded segment of length l, orientation angle, θ, with respect to the loading direction. Owing to the snubbing-friction effect, the pull-out load is [6, 7, 17, 35, 36]

$$P(l, s, \theta) = \tau_f(s)\pi d_f(l - s)\exp(\mu\theta) \tag{23}$$

where s is the slippage distance of the embedded end of the fibre. If the fibre is inextensible, then the crack-opening displacement is identical to the slip length, i.e. $\delta = s$. Then the fibre pull-out load is

$$P(l, \delta, \theta) = \tau_f(\delta)\pi d_f(l - \delta)\exp(\mu\theta) \quad \text{for } l \geqslant \delta \tag{24a}$$

$$P(l, \theta, \delta) = 0 \quad \text{for } l < \delta \tag{24b}$$

Thus the energy absorption for a single fibre of embedded length, l, pulled out at an angle θ is given by

$$w_{po}(l, \theta) = \int_{\delta=0}^{l} P(l, \delta, \theta)\,d\delta$$

$$= [(a_0 l^2/2) + (a_1 l^3/6) + (a_2 l^4/12)]\pi d_f \exp(\mu\theta)$$

$$\text{for } l < L_{c\theta}/2 \tag{25}$$

$$w_{po}(l, \theta) = 0 \quad \text{for } l \geqslant L_{c\theta}/2 \tag{26}$$

where $L_{c\theta}$ is the critical fibre length for an oblique fibre pulled out at an angle, θ, with the loading direction [33]. In the case $l \geqslant L_{c\theta}/2$, the fibre will break instead of being pulled out. $L_{c\theta}$ can be expressed as

$$L_{c\theta} = \sigma_{fu\theta} d_f/[2\tau_i \exp(\mu\theta)] \tag{27}$$

where $\sigma_{fu\theta}$ is the fracture stress of oblique fibres [27, 28, 30] or the so-called fibre inclined strength [29]. For brittle fibres the fracture stress of oblique fibres is given by [27, 28]

$$\sigma_{fu\theta} = \sigma_{fu}(1 - A\tan\theta) \tag{28}$$

where A is a constant determining the fibre inclined strength. The critical transfer length of aligned fibres, L_c, is defined by Equation 1, therefore $L_{c\theta}$ can be rewritten as

$$L_{c\theta} = L_c(1 - A\tan\theta)/\exp(\mu\theta) \tag{29}$$

2.4. Pull-out energy of short fibre composites

Now we consider a rectangular-shaped specimen with the lengths of the three mutually perpendicular edges denoted by c_1, c_2 and c_3. The c_3 axis is chosen to be parallel to the loading direction. A_c and A_f are assumed to be the cross-sectional areas of the specimen and that of the fibre, respectively. V_f and $\bar{L}$ are the fibre volume fraction and the mean fibre length. The total number of fibres in the specimen is

$$N = A_c c_3 V_f/(A_f \bar{L}) \tag{30}$$

The fibre-length distribution and the fibre-orientation distribution are assumed to be independent, so the number of fibres of a length between L and $L + \mathrm{d}L$ and an angle from θ to $\theta + \mathrm{d}\theta$ is given by

$$\mathrm{d}N = Nf(L)g(\theta)\,\mathrm{d}L\,\mathrm{d}\theta \tag{31}$$

The fibres are assumed to be distributed uniformly in the composite, so the number, $\mathrm{d}N_c$, of the fibres of a length from L to $L + \mathrm{d}L$ and an angle from θ to $\theta + \mathrm{d}\theta$, which crosses any cross-section of the composite, is

$$\mathrm{d}N_c = \mathrm{d}NL\cos(\theta)/c_3 \tag{32}$$

Then the number of fibres with a shorter embedded length between l and $l + \mathrm{d}l$ across any cross-section of the composite is

$$\mathrm{d}N_c(l) = \mathrm{d}N_c[\mathrm{d}l/(L/2)] \tag{33}$$

Because of the snubbing-friction effect and the fibre inclined strength effect, the critical fibre embedded length is reduced by a factor $(1 - A\tan\theta)/\exp(\mu\theta)$ (see Equation 29); this accounts for the misalignment of the fibre with respect to the applied load. Any fibre with orientation θ whose shorter embedded segment has a length of $l \geqslant L_{c\theta}/2$ will break. Then a step function can be defined for accounting for fibre breakage

$$U(l) = \begin{cases} 1 & \text{for } l < L_{c\theta}/2 \\ 0 & \text{for } l \geqslant L_{c\theta}/2 \end{cases} \tag{34}$$

The fibre pull-out energy of composites is then given by

$$w_{po} = (1/A_c)\int_{\theta=0}^{\pi/2}\int_{L=L_{min}}^{L_{max}}\int_{l=0}^{L/2} w_{po}(l,\theta)U(l)Nf(L) \times g(\theta)(L\cos(\theta)/c_3)(2/L)\,\mathrm{d}l\,\mathrm{d}L\,\mathrm{d}\theta \tag{35}$$

For a constant fibre length case, Equation 35 becomes

$$w_{po} = (1/A_c)\int_{\theta=0}^{\pi/2}\int_{l=0}^{L/2} w_{po}(l,\theta)U(l)Ng(\theta) \times (L\cos(\theta)/c_3)(2/L)\,\mathrm{d}l\,\mathrm{d}\theta \tag{36}$$

The step function $U(l)$ has been included in the integrand to discount those fibres which will be broken instead of being pulled out, so the step function effectively changes the limits of integration. The percentage, α, of the fibres of lengths greater than $L_{c\theta}$ is given by

$$\alpha = 1 - \int_0^{\pi/2}\int_{L_{min}}^{L_{c\theta}} f(L)g(\theta)\,\mathrm{d}L\,\mathrm{d}\theta \tag{37}$$

and the fibre-orientation angle has a limit θ_{max} according to Equation 28 for $\sigma_{fu\theta} \geqslant 0$

$$\theta_{max} = \arctan(1/A) \tag{38}$$

Considering Equation 30, Equation 36 can be rewritten as

$$w_{po1} = \left(\frac{2V_f}{A_f\bar{L}}\right)\left[\int_{\theta=0}^{\theta_{max}}\int_{l=0}^{L/2} w_{po}(l,\theta)g(\theta)\cos(\theta)\,\mathrm{d}l\,\mathrm{d}\theta\right] \quad \text{for } L \leqslant L_{c\theta_{max}} \tag{39a}$$

$$w_{po2} = \left(\frac{2V_f}{A_f\bar{L}}\right)\left[\int_{\theta=\theta_0}^{\theta_{max}}\int_{l=0}^{L_{c\theta}/2} w_{po}(l,\theta)g(\theta)\cos(\theta)\,\mathrm{d}l\,\mathrm{d}\theta + \int_{\theta=0}^{\theta_0}\int_{l=0}^{L/2} w_{po}(l,\theta)g(\theta)\cos(\theta)\,\mathrm{d}l\,\mathrm{d}\theta\right] \quad \text{for } L_{c\theta_{max}} < L < L_c \tag{39b}$$

$$w_{po3} = \left(\frac{2V_f}{A_f\bar{L}}\right)\left[\int_{\theta=0}^{\theta_{max}}\int_{l=0}^{L_{c\theta}/2} w_{po}(l,\theta)g(\theta)\cos(\theta)\,\mathrm{d}l\,\mathrm{d}\theta\right] \quad \text{for } L \geqslant L_c \tag{39c}$$

where θ_0 and $L_{c\theta_{max}}$ can be determined from the following equations

$$(1 - A\tan\theta_0)\exp(-\mu\theta_0) = L/L_c \tag{40}$$

$$L_{c\theta_{max}} = L_c(1 - A\tan\theta_{max})\exp(-\mu\theta_{max}) \tag{41}$$

So the fibre pull-out energy of a composite with a fibre length distribution $f(L)$ can finally be obtained by superposition

$$w_{po} = \int_0^{L_{c\theta_{max}}} w_{po1}f(L)\,\mathrm{d}L + \int_{L_{c\theta_{max}}}^{L_c} w_{po2}f(L)\,\mathrm{d}L + \int_{L_c}^{L_{max}} w_{po3}f(L)\,\mathrm{d}L \tag{42}$$

However, θ_0 cannot be solved directly from Equation 40 when $A \neq 0$, so it is not suitable as a limit of integration if we would like to evaluate the fibre pull-out energy from Equation 42 using a computer program, for example *Mathematica*. To avoid this inconvenience, another method to derive the pull-out energy will be given. For a constant orientation angle case, if $L < L_{c\theta}$, the lower and upper integration limits of l are 0 and $L/2$; on the other hand, if $L \geqslant L_{c\theta}$, the lower and upper integration limits of l are 0 and $L_{c\theta}/2$. Then, for a constant angle case, Equation 35 can be rewritten as

$$w_{po4} = \left(\frac{2V_f}{A_f\bar{L}}\right)\int_{L_{min}}^{L_{c\theta}}\int_{l=0}^{L/2} w_{po}(l,\theta)f(L)\cos(\theta)\,\mathrm{d}l\,\mathrm{d}L \quad \text{for } L < L_{c\theta} \tag{43}$$

$$w_{po5} = \left(\frac{2V_f}{A_f\bar{L}}\right)\int_{L_{c\theta}}^{L_{max}}\int_{l=0}^{L_{c\theta}/2} w_{po}(l,\theta)f(L)\cos(\theta)\,\mathrm{d}l\,\mathrm{d}L \quad \text{for } L \geqslant L_{c\theta} \tag{44}$$

So we can obtain the fibre pull-out energy

$$w_{po} = \int_{\theta=0}^{\theta_{max}}(w_{po4} + w_{po5})g(\theta)\,\mathrm{d}\theta \tag{45}$$

i.e.

$$w_{po} = \left(\frac{2V_f}{A_f\bar{L}}\right)\left[\int_{\theta=0}^{\theta_{max}}\int_{L=L_{min}}^{L_{c\theta}}\int_{l=0}^{L/2} w(l,\theta)f(L)g(\theta) \times \cos(\theta)\,dl\,dL\,d\theta + \int_{\theta=0}^{\theta_{max}}\int_{L=L_{c\theta}}^{L_{max}}\int_{l=0}^{L_{c\theta}/2} w(l,\theta)\,f(L)g(\theta) \times \cos(\theta)\,dl\,dL\,d\theta\right] \quad (46)$$

For $A = 0$, it is easy to determine that Equations 42 and 46 give identical results. When $A \neq 0$, θ_0 cannot be solved directly from Equation 40 and is then unsuitable to be a limit of integration; thus Equation 42 is not used for evaluating w_{po}. However, Equation 46 can be used easily to evaluate the fibre pull-out energy of short fibre composites. Equation 46 can be rewritten as

$$w_{po} = \frac{8V_f a_0}{d_f\bar{L}}\left[\int_{\theta=0}^{\theta_{max}}\int_{L=L_{min}}^{L_{c\theta}}\int_{l=0}^{L/2}\left(\frac{l^2}{2}+\frac{a_1 l^3}{6a_0}+\frac{a_2 l^4}{12a_0}\right) \times f(L)g(\theta)\cos(\theta)\exp(\mu\theta)\,dl\,dL\,d\theta + \int_{\theta=0}^{\theta_{max}}\int_{L=L_{c\theta}}^{L_{max}}\int_{l=0}^{L_{c\theta}/2}\left(\frac{l^2}{2}+\frac{a_1 l^3}{6a_0}+\frac{a_2 l^4}{12a_0}\right) \times f(L)g(\theta)\cos(\theta)\exp(\mu\theta)\,dl\,dL\,d\theta\right] \quad (47)$$

For a unidirectional composite with fibres of a length $L < L_c$, the fibre pull-out energy can be deduced from Equation 47 by neglecting the fibre-length and fibre-orientation distributions

$$w_{po} = \frac{V_f \tau_f L^2}{6d_f} \qquad \text{for } L < L_c \quad (48)$$

Equation 48 is the same as Equation 2. Moreover, if the inclined fibre strength effect is neglected, i.e. $A = 0$, then Equations 39a–c become

$$w_{po1} = \left(\frac{2V_f}{A_f\bar{L}}\right)\left[\int_{\theta=0}^{\pi/2}\int_{l=0}^{L/2} w_{po}(l,\theta)g(\theta)\cos(\theta)\,dl\,d\theta\right] \quad \text{for } L < L_c\exp(-\mu\pi/2) \quad (49a)$$

$$w_{po2} = \left(\frac{2V_f}{A_f\bar{L}}\right)\left[\int_{\theta=\theta_0}^{\pi/2}\int_{l=0}^{L_{c\theta}} w_{po}(l,\theta)g(\theta)\cos(\theta)\,dl\,d\theta + \int_{\theta=0}^{\theta_0}\int_{l=0}^{L/2} w_{po}(l,\theta)g(\theta)\cos(\theta)\,dl\,d\theta\right] \quad \text{for } L_c > L \geqslant L_c\exp(-\mu\pi/2) \quad (49b)$$

$$w_{po3} = \left(\frac{2V_f}{A_f\bar{L}}\right)\left[\int_{\theta=0}^{\pi/2}\int_{l=0}^{L_{c\theta}/2} w_{po}(l,\theta)g(\theta)\cos(\theta)\,dl\,d\theta\right] \quad \text{for } L \geqslant L_c \quad (49c)$$

where $\theta_0 = \ln(L/L_c)/\mu$ and $L_{c\theta} = L_c/\exp(\mu\theta)$; $g(\theta)$ is equivalent to $\sin\theta h(\theta)$ defined by Wetherhold and Jain [6, 7] (see Equations 10–12). From Equations 49a–c, Equations 9a–c can be derived, and this limiting case was studied by Wetherhold and Jain [6].

Equations 48 and 49a–c show that within the present model, the previously existing fibre pull-out energy theories are included as special cases.

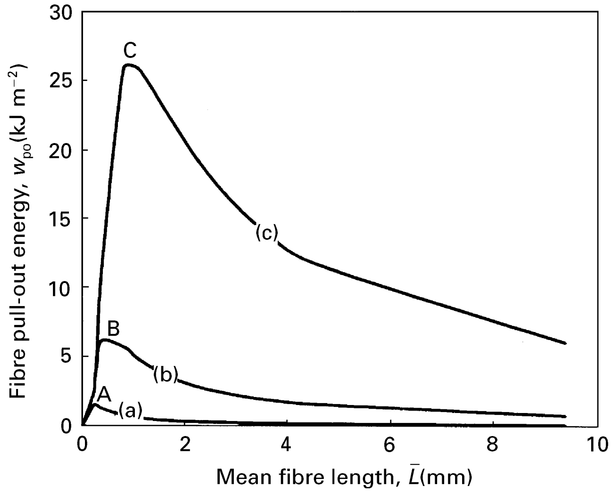

Figure 3 Fibre pull-out energy versus mean fibre length for (a) $L_c = 0.376$ mm, (b) $L_c = 0.837$ mm, (c) $L_c = 1.71$ mm.

3. Results and discussion

Based on Equation 47 the fibre pull-out energy can be predicted. The effects of mean fibre length and critical fibre transfer length on the fibre pull-out energy are shown in Fig. 3, where $\mu = A = 0.25$, $\bar{\theta} = 0.589$ radian ($p = 1$ and $q = 2$), $L_{mod} = 0.2$ mm, $d_f = 10\ \mu$m, $V_f = 0.20$, $\tau_f = a_0 = 10\ \text{MN m}^{-2}$ (assuming a constant interfacial frictional shear stress case by letting $a_1 = a_2 = 0$) and various L_c. Under a given critical fibre length, the fibre pull-out energy increases with the mean fibre length until a certain value slightly less than the critical transfer length L_c, at which the maximum of fibre pull-out energy is reached (see points A, B and C in the curves). This is because the pull-out energy is contributed by subcritical fibres of lengths less than $L_{c\theta}$ and supercritical fibres of lengths greater than $L_{c\theta}$, the sum of the two parts reaches the maximum at a certain mean fibre length slightly less than $L_{c\theta}$. Afterwards, the fibre pull-out energy decreases with the mean fibre length, because more fibres will rupture and will not contribute to the fibre pull-out energy. For different critical fibre length cases the fibre pull-out energy increases with the critical fibre length. When $L_c = 0.376$ mm, the maximum fibre pull-out energy is less than $1.5\ \text{kJ m}^{-2}$; however, when $L_c = 1.71$ mm, the fibre pull-out energy is large and greater than $22\ \text{kJ m}^{-2}$ when the mean fibre length is between about 0.85 and 1.75 mm. So, a large critical fibre length is very efficient for achieving a high fibre pull-out energy. This can be further shown by Table I for $L_c = 9.371$ mm; the fibre pull-out energy can be very large, e.g. $1373.66\ \text{kJ m}^{-2}$ at $L = \bar{L} = 9.371$ for a undirectional fibre composite case and $476.20\ \text{kJ m}^{-2}$ at $L = \bar{L}$ for a randomly aligned fibre composite case. However, in experiments, such large fracture energies of short fibre composites were scarcely attained; this may be because such large critical fibre lengths were scarcely achieved. In summary, when the mean fibre length is small, the fibre pull-out energy is small, no matter how large the critical fibre length; when the mean fibre length is comparatively large (e.g. about 1 mm in this study), the fibre pull-out energy would be large if the critical fibre length could

TABLE I Fibre pull-out energy versus mean fibre length for $L_c = 9.371$ mm

$\bar{L}$ (mm)	w_{po} (kJ m^{-2}) $\bar{\theta} = 0.785$	$\bar{\theta} = 0$
0.218	1.76	2.29
0.241	2.50	3.53
0.279	3.93	5.56
0.376	9.01	12.76
0.837	63.91	93.32
1.710	256.59	447.06
9.371	476.20	1373.66

TABLE II The effect of fibre diameter, d_f on fibre pull-out energy

Mean fibre length, $\bar{L}$ (mm)	Fibre pull-out energy (kJ m^{-2})		
	$d_f = 3.76$ μm	$d_f = 8.37$ μm	$d_f = 17.1$ μm
0.218	3.88	2.68	1.33
0.241	3.96	3.68	1.88
0.279	3.86	5.20	2.95
0.376	3.30	7.31	6.38
0.837	1.84	6.70	15.12
1.119	1.42	5.66	15.12
1.710	0.98	4.18	13.11
2.315	0.74	3.29	11.12
2.935	0.59	2.69	9.51
3.564	0.49	2.27	8.26
4.515	0.39	1.84	6.88
9.371	0.19	0.90	3.54

be large (see curve c), otherwise the fibre pull-out energy would be small (see curve a). From Equation 1 it can be seen that the critical fibre length is proportional to the fibre tensile strength and inversely proportional to the interfacial shear stress; therefore, high-strength fibres and a weakly bonded interface are conducive to obtaining a high fibre pull-out energy. Moreover, the critical fibre length is proportional to the fibre diameter (see Equation 1); however, the variation of fibre pull-out energy with fibre diameter cannot be shown only from this point, because the expression for fibre pull-out energy (see Equation 47) contains a term of $1/d_f$. Table II shows the effect of fibre diameter on the fibre pull-out energy for the case of $L_c = 0.837$ mm. It can be concluded from Table II that a smaller fibre diameter corresponds to a higher fibre pull-out energy when the mean fibre length is small; however, for the case of large mean fibre length, a larger fibre diameter corresponds to a higher fibre pull-out energy.

Fig. 4 shows the effect of mean fibre-orientation angle, $\bar{\theta}$, or fibre-orientation coefficient, f_θ, on the fibre pull-out energy, where $\mu = A = 0.25$, $L_c = 1.71$ mm, $L_{mod} = 0.2$ mm, $d_f = 10$ μm, $V_f = 0.20$, $\tau_f = 10$ MN m^{-2} and various $\bar{\theta}$ (i.e. 0, 0.589 and 0.785 rad) or f_θ (i.e. 1, 0.33 and 0). Fig. 4 reveals that the fibre pull-out energy decreases with the increase of mean fibre-orientation angle, $\bar{\theta}$, or the decrease of f_θ. For the randomly distributed fibre case, $\bar{\theta} = 0.785$ rad or $f_\theta = 0$, the maximum (about 20 kJ m^{-2}) is attained at the vicinity of $\bar{L} = 0.873$ mm. For the unidirectional

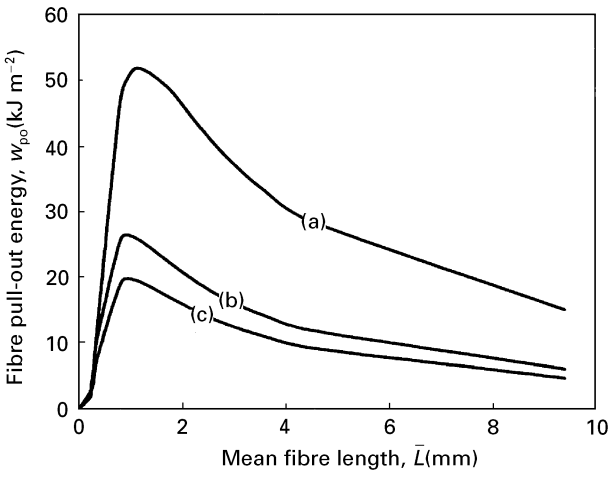

Figure 4 Fibre pull-out energy versus mean fibre length for (a) $\bar{\theta} = 0$ or $f_\theta = 1$, (b) $\bar{\theta} = 0.589$ or $f_\theta = 0.33$; (c) $\bar{\theta} = 0.785$ or $f_\theta = 0$.

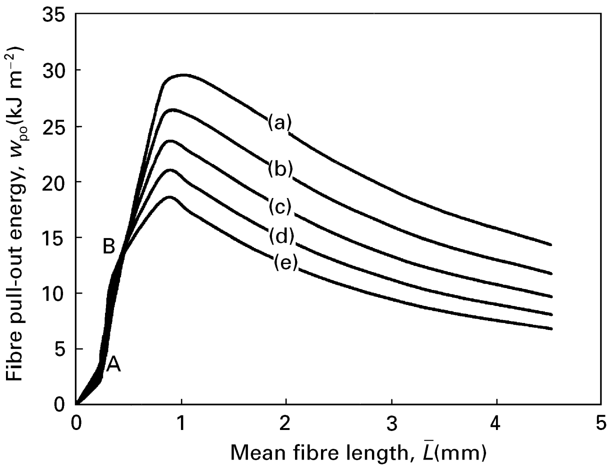

Figure 5 Fibre pull-out energy versus mean fibre length for various μ: (a) μ = 0, (b) μ = 0.25, (c) μ = 0.5, (d) μ = 0.75, (e) μ = 1.

fibre composite case, i.e. $\bar{\theta} = 0$ radian or $f_\theta = 1$, the fibre pull-out energy reaches the maximum (52 kJ m^{-2}) at $\bar{L} = 1.2$ mm and the fibre pull-out energy is about 47 kJ m^{-2}at $\bar{L} = 0.873$. So, for a given fibre–matrix system, the unidirectional fibre composite case gives the highest fibre pull-out energy if the crack propagates perpendicular to the fibres.

The effect of snubbing friction on the fibre pull-out energy is shown by Fig. 5, where $A = 0.25$, $L_{mod} = 0.2$ mm, $d_f = 10$ μm, $V_f = 0.20$, $L_c = 1.71$ mm, $\tau_f = 10$ MN m^{-2}, $\bar{\theta} = 0.589$ and various μ. When the mean fibre length is small (e.g. $\bar{L} < 0.837$ mm), the fibre pull-out energy increases with the snubbing-friction coefficient, because the pull-out load is increased by the snubbing-friction effect. As the mean fibre length increases to a certain value, the fibre pull-out energy is the same for two different μ (see the crossing points A and B, etc., in the curves). This can be explained as follows. The fibre pull-out load is increased by increasing the snubbing-friction coefficient; on the other hand, the number of fibres active in the bridging action reduces due to the fact that more fibres will break by increasing μ, when the two competing effects balance out, the fibre pull-out energy is

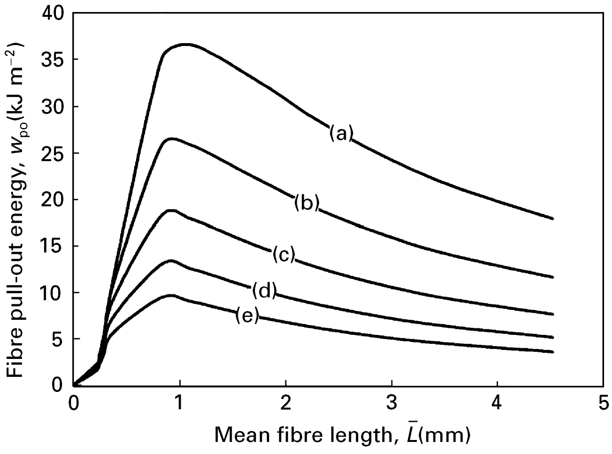

Figure 6 Fibre pull-out energy versus mean fibre length for (a) $A = 0$, (b) $A = 0.25$, (c) $A = 0.5$, (d) $A = 0.75$, (e) $A = 1$.

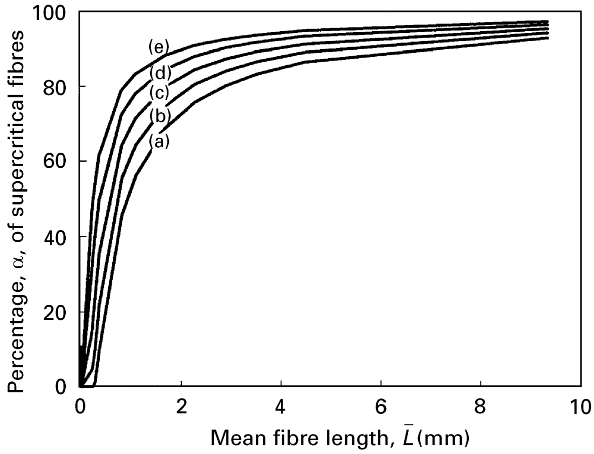

Figure 7 Percentage of supercritical fibres of lengths greater than L_{c0} for (a) $A = 0$, (b) $A = 0.25$, (c) $A = 0.5$, (d) $A = 0.75$, (e) $A = 1$.

TABLE III Fibre pull-out energy (kJ m^{-2}) versus mode fibre length (mm) for $\bar{L} = 1$ and 0.2 mm

$\bar{L} = 1$ mm		$\bar{L} = 0.2$ mm	
L_{mod}	w_{po}	L_{mod}	w_{po}
0.1172	25.62	0.0234	1.12
0.2388	26.41	0.0478	0.95
0.3505	27.08	0.0701	0.83
0.4484	27.65	0.0897	0.73
0.5326	28.15	0.1065	0.66
0.6042	28.57	0.1208	0.60
0.7166	29.25	0.1433	0.52

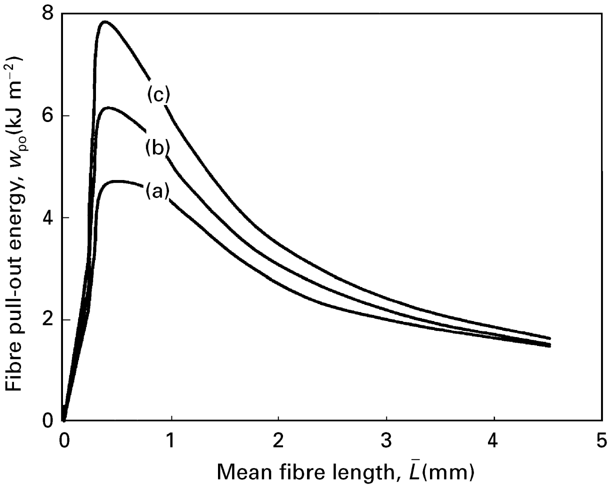

Figure 8 Fibre pull-out energy versus mean fibre length for (a) slip-softening, $a_0 = 10$ MN m^{-2}, $a_1 = [-1.245a_0/(L/2)]$, $a_2 = [0.395a_0/(L/2)^2]$; (b) constant interfacial frictional shear stress, $a_0 = 10$ MN m^{-2}; (c) slip hardening, $a_0 = 10$ MN m^{-2}, $a_1 = 2a_0/L$, $a_2 = a_0/(L/2)^2$.

the same for two different μ. When the mean fibre length is large, the fibre pull-out energy decreases with the snubbing-friction coefficient, because for large mean fibre-length cases, more fibres will fracture and do not contribute to the fibre pull-out energy.

Fig. 6 shows the effect of the parameter A on the fibre pull-out energy, where $\mu = 0.25$, $L_{mod} = 0.2$ mm, $d_f = 10$ μm, $V_f = 0.20$, $L_c = 1.71$ mm, $\tau_f = 10$ MN m^{-2}, $\bar{\theta} = 0.589$ and various A. As the curves show, the fibre pull-out energy decreases with the increase of parameter A. This can be explained by Fig. 7 which expresses the effect of A on the percentage of supercritical fibres of lengths greater than $L_{c\theta}$. Because the percentage of supercritical fibres increases with parameter A, the percentage of the fibres which will fracture and do not contribute to the fibre pull-out energy will increase with A, therefore w_{po} decreases with A.

Table III shows the effect of mode fibre length on the fibre pull-out energy, where $\mu = A = 0.25$, $L_c = 1.71$ mm, $\bar{L} = 1$ and 0.2 mm, $d_f = 10$ μm, $V_f = 0.20$, $\tau_f = 10$ MN m^{-2}, $\bar{\theta} = 0.589$ and various L_{mod}. It can be seen from Table III that the fibre pull-out energy increases slightly with the mode fibre length when the mean fibre length is large (e.g. $\bar{L} = 1$ mm) and decreases with L_{mod} when the mean fibre length is small (e.g. $\bar{L} = 0.2$ mm).

The fibre pull-out energy is shown in Fig. 8 for the cases of slip softening, constant interfacial frictional shear stress and slip hardening, where $\mu = A = 0.25$, $L_{mod} = 0.2$ mm, $d_f = 10$ μm, $V_f = 0.20$, $L_c = 0.837$ mm and $\bar{\theta} = 0.589$. The condition that there is no pull-out of the longer embedded segments will be satisfied if Equations 7 and 8 are satisfied. For the cases of constant τ_f and slip softening, this condition will be satisfied automatically. For satisfying this condition the slip-hardening interface is represented by $a_1/a_0 = 2L$, $a_2/a_0 = (2/L)^2$. It can be seen from Fig. 8 that the case of slip hardening corresponds to the comparatively large fibre pull-out energy, the case of constant τ_f to the moderate fibre pull-out energy, and the case of slip softening to the comparatively small fibre pull-out energy.

Additionally, it can be seen from Equation 47 that as the fibre-volume fraction and the interfacial frictional shear stress (assuming a constant interfacial frictional shear stress case) increase, the fibre pull-out energy will increase proportionally. Thus, in order to achieve a high fibre pull-out energy and hence a high fracture toughness of short fibre composites, a high interfacial frictional shear stress and a high fibre-volume fraction are favourable. But, as the fibre-volume fraction increases, the matrix-volume fraction will decrease, so the toughness contribution of matrix-related mechanisms will reduce. The two competing effects may result in an optimum fibre-volume fraction for the maximum fracture toughness for some short fibre composites in which both the matrix and fibres are active in contributing to the fracture toughness of composites (see [20]). However, this was not the purpose of the present study.

4. Conclusion

The fibre pull-out energy has been studied for short fibre composites in which there are fibre-length and fibre-orientation distributions. The results have shown that a large mean fibre length may result in a high fibre pull-out energy if the critical fibre length is large; otherwise the fibre pull-out energy is comparatively small. The high-strength fibres, the weakly bonded interface between fibres and matrix, the low mean fibre-orientation angle and the small value of the parameter A for determining the inclined strength of fibres, are conducive to achieving a high fibre pull-out energy. A smaller fibre diameter corresponds to a higher fibre pull-out energy when the mean fibre length is small, while a large fibre diameter is beneficial to obtaining a high fibre pull-out energy when the mean fibre length is large. A larger snubbing-friction coefficient corresponds to a higher fibre pull-out energy when the mean fibre length is small, while a small snubbing-friction coefficient is beneficial to obtaining a high fibre pull-out energy for the large mean fibre length case. Slip-hardening cases give a higher fibre pull-out energy than that of corresponding constant interfacial frictional shear stress cases, and slip-softening cases give a lower fibre pull-out energy than that of corresponding constant interfacial frictional shear stress cases. Moreover, a comparatively high fibre-volume fraction and a large interfacial frictional shear stress are favourable to achieving a high fibre pull-out energy. The fibre pull-out energy increases slightly with the mode fibre length when the mean fibre length is large, while the fibre pull-out energy decreases with the mode fibre length when the mean fibre length is small.

Acknowledgement

The authors thank the Alexander von Humboldt foundation for financially supporting this work.

References

1. J. K. KIM and Y. W. MAI, *Compos. Sci. Technol.* **41** (1991) 333.
2. B. LAUKE, B. SCHULTRICH and R. BARTHEL, *ibid.* **23** (1985) 21.
3. B. LAUKE and W. POMPE, *ibid.* **26** (1986) 37.
4. B. LAUKE and B. SCHULTRICH, *ibid.* **26** (1986) 1.
5. B. LAUKE and W. POMPE, *ibid.* **31** (1988) 25.
6. R. C. WETHERHOLD and L. K. JAIN, *Mater. Sci. Eng.* **A151** (1992) 169.
7. L. K. JAIN and R. C. WETHERHOLD, *Acta Metall. Mater.* **40** (1992) 1135.
8. V. B. GUPTA, R. K. MITTAL and M. GOEL, *Compos. Sci. Technol.* **37** (1990) 353.
9. K. FRIEDRICH, *ibid.* **22** (1985) 43.
10. N. SATO, T. KURAUCHI, S. SATO and O. KAMIGAITO, *J. Mater. Sci.* **26** (1991) 3891.
11. H. BIJSTERBOSCH and R. J. GAYMANS, *Polym. Compos.* **16** (1995) 363.
12. J. L. HELFET and B. HARRIS, *J. Mater. Sci.* **7** (1972) 494.
13. G. A. COOPER and A. KELLY, "Interfaces in Composites", ASTM STP-452 (American Society for Testing and Materials, Philadelphia, PA, 1969) p. 90.
14. G. A. COOPER, *J. Mater. Sci.* **5** (1970) 645.
15. A. KELLY, *Proc. R. Soc. Lond.* **A319** (1970) 95.
16. Y. WANG, V. C. LI and S. BACKER, *Int. J. Cement Compos. Light Weight Concr.* **10** (1988) 143.
17. V. C. LI, Y. WANG and S. BACKER, *Composites* **21** (1990) 132.
18. R. TURKOVICH and L. ERWIN, *Polym. Eng. Sci.* **23** (1983) 743.
19. V. B. GUPTA, R. K. MITTAL and P. K. SHARMA, *Polym. Compos.* **10** (1989) 8.
20. B. LAUKE, B. SCHULTRICH and W. POMPE, *Polym. Plast. Technol. Eng.* (*Special Issue*) **29** (1990) 607.
21. T. VU-KHANH, J. DENAULT, P. HABIB and A. LOW, *Compos. Sci. Technol.* **40** (1991) 423.
22. P. J. HINE, N. DAVIDSON, R. A. DUCKETT and I. M. WARD, *ibid.* **53** (1995) 125.
23. M. XIA, H. HAMADA and Z. MAEKAWA, *Int. Polym. Process.* **5** (1995) 74.
24. W. K. CHIN, H. T. LIU and Y. D. LEE, *Polym. Compos.* **9** (1988) 27.
25. M. J. CARLING and J. G. WILLIAMS, *ibid.* **11** (1990) 307.
26. S. R. DOSHI and J. M. CHARRIER, *ibid.* **10** (1989) 28.
27. M. R. PIGGOTT, *J. Mech. Phys. Solids* **22** (1974) 457.
28. *Idem*, *J. Compos. Mater.* **28** (1994) 588.
29. P. J. M. BARTOS and M. DURIS, *Composites* **25** (1994) 945.
30. J. MORTON and G. W. GROVES, *J. Mater. Sci.* **11** (1976) 617.
31. F. ULRYCH, M. SOVA, J. VOKROUHLECKY and B. TURCIC, *Polym. Compos.* **14** (1993) 229.
32. K. TAKAHASHI and N. S. CHOI, *J. Mater. Sci.* **26** (1991) 4648.
33. S. Y. FU and B. LAUKE, *Compos. Sci. Technol.* **56** (1996) 1179
34. P. A. TEMPLETON, *J. Reinf. Plast. Compos.* **9** (1990) 210.
35. S. Y. FU, B. L. ZHOU and C. W. LUNG, *Smart Mater. Struct.* **1** (1992) 180.
36. S. Y. FU, S. H. LI, S. X. LI, B. L. ZHOU, G. H. HE and C. W. LUNG, *Script Metall. Mater.* **29** (1993) 1541.

Received 23 February
and accepted 17 September 1996